Multifunctional ferrimagnetic-ferroelectric thin films for microwave applications

R. Heindl, H. Srikanth,[a] S. Witanachchi, P. Mukherjee, A. Heim, and G. Matthews
Department of Physics, University of South Florida, Tampa, Florida 33620

S. Balachandran, S. Natarajan, and T. Weller
Department of Electrical Engineering, University of South Florida, Tampa, Florida 33620

(Received 1 February 2007; accepted 30 May 2007; published online 20 June 2007)

Ferrimagnetic and ferroelectric structures based on barium strontium titanate and barium hexaferrite are investigated for potential applications in tunable microwave devices. Thin film bilayers were grown on MgO and sapphire, and their underlying crystallographic, microstructural, and magnetic properties were analyzed and compared. Microcircuits were fabricated using optical lithography, and microwave properties and electrical tunability were measured in the range of 1–50 GHz. Overall, the studies demonstrate the possibility of realizing high quality multifunctional microwave materials that combine tunable magnetic and dielectric properties. © *2007 American Institute of Physics*. [DOI: 10.1063/1.2750519]

The combination of desirable microwave response of ferrites and ferroelectrics in monolithic layered thin film heterostructures is of topical interest given the thrust for integrated functionalities in microwave devices. This study focuses on ferrite-ferroelectric thin film bilayers aimed at such applications.

The materials of our choice, ferroelectric $Ba_{0.5}Sr_{0.5}TiO_3$ (BST) and *M*-type hexaferrite $BaFe_{12}O_{19}$ (BaM), for the bilayers are both well studied and used in many microwave applications and have shown excellent properties in this region of the electromagnetic spectrum.[1–4]

Over the past few years, there has been an increase in interest in electrically and magnetically tunable materials operating at microwave frequencies. However, the majority of the studies are limited to low frequencies (below 10 GHz) or many of the investigated samples have one of the components (ferrite or ferroelectric) in the bulk form.[5–7] In this letter, we report on high quality bilayer films grown on MgO and sapphire substrates using pulsed laser deposition (PLD). Along with the structural and magnetic properties, we also demonstrate the electrical tunability at microwave frequencies up to 50 GHz.

Bilayer thin films of BaM and BST were grown on polished C-oriented sapphire and (100)-MgO substrates using pulsed laser deposition, with energy densities of the KrF excimer laser spot at the target surface being around 8.7 and 4.3 J/cm^2 for BaM and BST targets, respectively. The substrates were positioned 5.5 cm away from the target and parallel to the target surface. The laser pulse rate was increased from 1 to 10 pulse/s gradually over the first 10 min of the deposition, and then kept at 10 pulse/s. The substrate temperature was maintained at around 650 °C using a heater and conductive silver paste at the substrate-heater interface. From our past experience and published literature from other groups, it is known that the ideal deposition temperature for BaM on sapphire is around 920 °C,[8] while the ideal deposition temperature for BST varies from 775 to 820 °C.[9,10] The maximum deposition temperature with this setup was 650 °C generated by a quartz lamp so this was the temperature in our depositions. All depositions were done at 250 mtorr pressure of high purity O_2. After the deposition, the films were cooled *in situ* to room temperature at a rate of 5 °C/min at 1 atm gas pressure. Subsequently, all films were postannealed *ex situ* in a quartz tube furnace in flowing O_2 at 900 °C for 8 h. The BaM was deposited using 45 000 pulses, resulting in a thickness of ≈500 nm, and the BST needed 61 000 pulses for the same thickness.

The x-ray diffraction patterns for the MgO‖BST‖BaM and sapphire‖BaM‖BST bilayers are shown in Fig. 1. The main panels show the intensity in log scale for the Θ-2Θ scan of the sample. The MgO‖BST‖BaM bilayer shows a

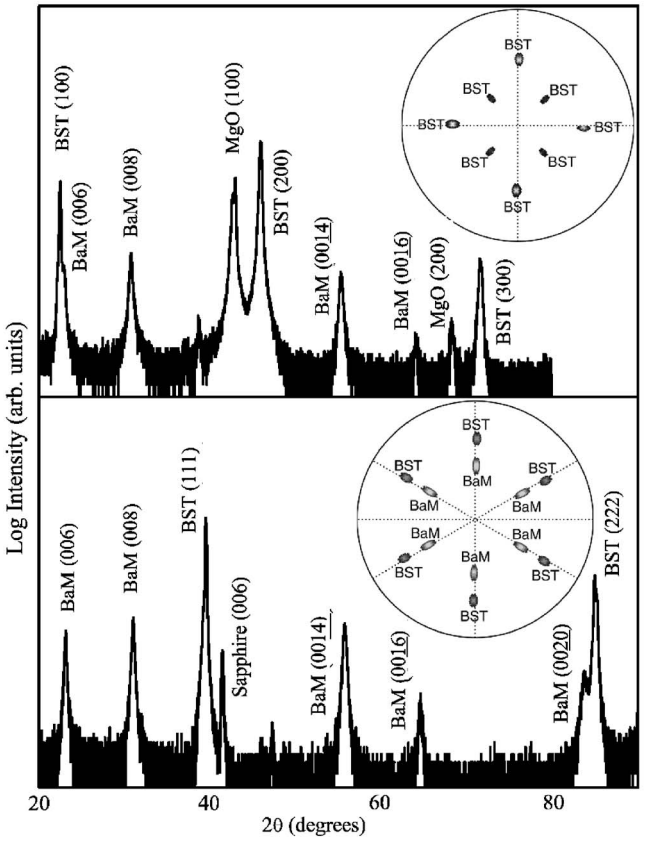

FIG. 1. Top: XRD pattern of MgO‖BST‖BaM bilayer. Bottom: XRD pattern of sapphire‖BaM‖BST bilayer thin films. Pole plots are shown in the insets.

[a]Electronic mail: sharihar@cas.usf.edu

(*h*00)-oriented BST film and a (00l)-oriented BaM film. The full width at half maximum (FWHM) of the rocking curve (not shown here) of BaM (008) peak is 0.55° and of BST (200) peak is 0.47°, indicating a high degree of planar orientation. The x-ray pole plot of the BST (220) peak (top inset) indicates the presence of two sets of four poles, consistent with the calculation of the interplanar angles, confirming that the BST film is single crystalline. Pole plot of BaM could not be measured due to the proximity of possible X-ray diffraction (XRD) peaks to the peaks of BST that have much higher intensity.

The sapphire‖BaM‖BST bilayer also shows a BaM film with only peaks belonging to the (00l) group of peaks, while the BST film shows a strong alignment in the (*hhh*) direction. The FWHMs of the rocking curves are 0.37° for BaM (008) peak and 0.41° for BST (111) peak, also confirming a good film orientation. The inset at the bottom shows the XRD pole plot of BaM (107) and BST (200) peaks. There are six peaks in the pole plot of the BaM film and also six peaks in the pole plot of the BST film. (111)-oriented BST has a threefold symmetry about the axis perpendicular to the plane.[11] Occurrence of six poles in the BST film indicates the presence of two sets of epitaxial single crystallites rotated by 60° to each other—$[(200),(020),(002),(\bar{2}00),(2\bar{0}0),(20\bar{0})]$. This is due to twinning that develops during film growth or cooling from high-temperature deposition to room temperature, when there is a large lattice mismatch.[12] Overall, the microstructure results indicate that the BST film is not purely single crystalline, but rather epitaxially polycrystalline. One set of three poles and one set of six poles of (111)-BST film grown on (111)-MgO were also observed by Moon *et al.*[13] In the case of BaM film, the six peaks come from the six sets of (107) planes associated with the six faces of the hexagon as BaM has a magnetoplumbite crystal structure. Every time the sample is rotated by 60° a Bragg condition is satisfied, resulting in a peak. This is consistent with epitaxial growth of BaM, with crystalline axis of BaM being parallel to the (00l) axis of sapphire, also reported in Ref. 14.

The room temperature magnetic hysteresis (*M-H*) curves are shown in Fig. 2. Comparison shows quite different magnetic responses in the two bilayer structures. The top panel shows that the MgO‖BST‖BaM bilayer is magnetically hard with $H_C \approx 2000$ Oe, and that the in-plane and out-of-plane magnetization loops do not show a significant preferential orientation. This is explained as a competition between crystal anisotropy trying to align the magnetization perpendicular to the plane and the shape anisotropy trying to align the magnetization in the film plane. This is also consistent with atomic force microscopy (AFM) images of the topmost surface of the bilayers. The AFM scan in the top inset shows the presence of characteristic acicular BaM crystallites, oriented in the film plane, which favor magnetization parallel to the film plane.[15] In contrast, a large out-of-plane anisotropy is observed in the sapphire‖BaM‖BST bilayer, typical for out-of-plane grown crystallites, with easy magnetization axis perpendicular to the film plane. The inset in the bottom panel shows the AFM scan of a sapphire‖BaM single layer (deposited under same conditions as the multilayer), revealing hexagonal crystallites growing out of the film plane, consistent with the magnetization studies. Large out-of-plane hysteresis is indication of higher microwave losses, most likely originating from the strain at the BaM‖BST interface.

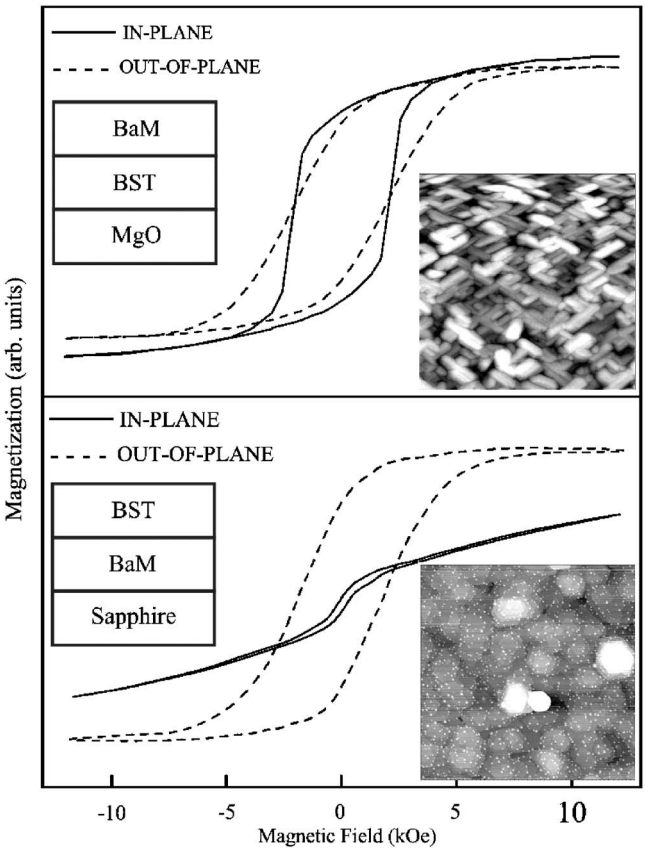

FIG. 2. Top: *M-H* loops of MgO‖BST‖BaM bilayer. Bottom: *M-H* loops of sapphire‖BaM‖BST bilayer thin films. AFM scans of the BaM layer and the stacking of the layers are shown in the insets.

Microwave measurements to test the electrical tunability of the bilayers were done with a probe station using an Anritsu 37397C vector network analyzer with integrated microwave source and *S*-parameter test set. A device that provides phase shift using coplanar waveguides (CPW) was employed. CPWs were fabricated on top of the bilayer structures using optical lithography. The thickness of the deposited metal layers was 15 nm of Cr and 1 μm of Au. The gap between the central and the ground lines was 5 μm. The width of the central line and the length of the CPW were 10.5 and 4200 μm for MgO‖BST‖BaM and 8.5 and 3000 μm for sapphire‖BaM‖BST bilayers, respectively. Reflection (S_{11}) and transmission (S_{21}) coefficients were measured after a careful short-open-load-through calibration. The voltage was applied using bias tees. Figure 3 shows the microwave response of the devices up to 50 GHz at various applied electrical fields. Above 50 GHz the calibration tends to become unreliable, but we observed that the linear increase of the phase shift continues up to at least 65 GHz which is the upper limit for the network analyzer.

The phase shift of the transmission coefficient S_{21} is described as[16]

$$\Delta\phi = \phi_2 - \phi_1 = \frac{360fl}{c}\left(\sqrt{\epsilon^2_{\text{eff}}\mu^2_{\text{eff}}} - \sqrt{\epsilon^1_{\text{eff}}\mu^1_{\text{eff}}}\right),$$

with f the operating frequency, l the length of the CPW line, c the speed of light, and "1" and "2" are the two different states (e.g., without and with bias field). As described by the above equation, the phase shift increases with frequency and applied voltage (increase in permittivity difference). This is

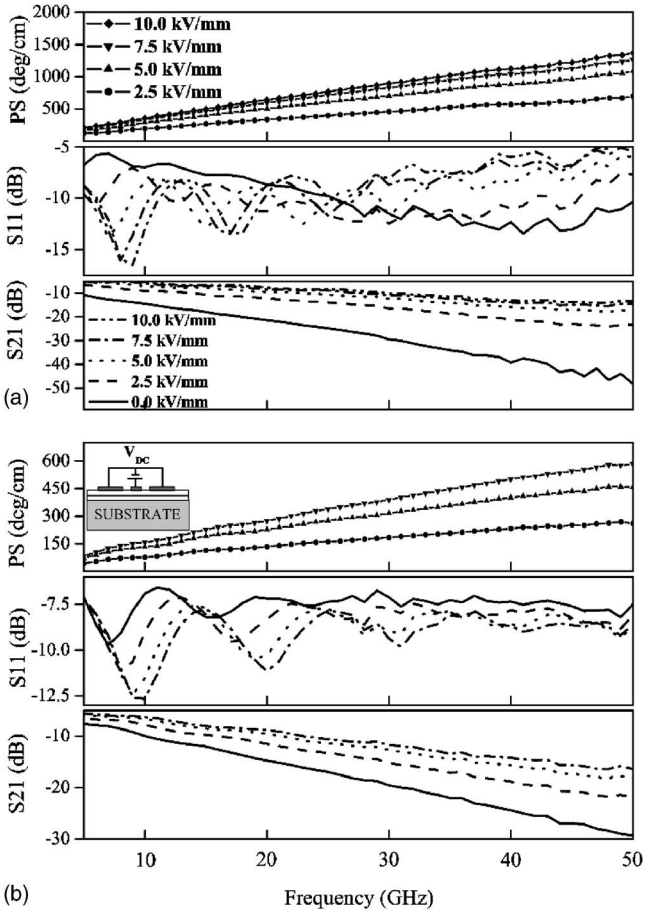

FIG. 3. Phase shift (°/cm), S_{11} (dB), and S_{21} (dB) of (a) MgO‖BST‖BaM and (b) sapphire‖BaM‖BST bilayer thin films. The inset shows a cross section of the CPW and the electrical biasing.

seen in Fig. 3, which plots the phase shift per unit length (°/cm) versus frequency. The MgO‖BST‖BaM bilayer has a higher tunability, probably because the BST film is single crystalline in this structure.

The *S* parameters of the measured structures as shown in Fig. 3 are not optimal from the perspective of phase-shifter design due to the continuous nature of the BST/BaM loading. There are two main aspects to consider, the low impedance of the CPW lines and the relatively small dimensions necessary for good field penetration. The CPW line dimensions provide a characteristic impedance of 50 Ω on bare MgO and sapphire substrates; however, the estimated characteristic impedance obtained with the BST/BaM layers present is 15–25 Ω depending on the bias condition, which results in high reflection loss. Also, the small dimensions of the lines increase current crowding and thus the insertion loss, a situation that is exacerbated by the low impedance (causing higher I^2R losses). From simulations, it was determined that at least 50% of the total insertion loss observed in the measured structures is attributable to conductor loss. Reflection loss accounts for decrease in S_{21} by 2–3 dB depending on the frequency and bias condition.

Despite the aforementioned effects, the phase of S_{21} remains a good indicator of the material's permittivity and permeability, as described by the above equation. The key observation is that electrical tunability is preserved in these bilayer structures and the presence of BaM affords an additional magnetic functionality which can be utilized in devices. The tunability of the phase shift (due to the ferrite response) using a magnetic field was also measured using a different device geometry; those results will be presented in a future paper and are beyond the scope of this letter.

The figures of merit (FOMs) of the devices are about 30°/dB for MgO‖BST‖BaM and 10°/dB for sapphire‖BaM‖BST at 7.5 kV/mm between 20 and 50 GHz. In comparison to topologies that are used for practical phase-shifter design, which utilize discrete tuning devices, and larger, lower loss interconnects between the devices,[17] the FOM here is relatively low. However, a similar study of a ferrimagnetic-ferroelectric tunable device that also used continuous loading reports on the electrical and magnetic tunabilities of BST films deposited on yttrium iron garnet bulk substrates.[6] The electrical phase shift was about 17°/cm at 10 GHz with 2.1 kV/mm, which is much smaller than the data obtained here. Thus we believe the results presented here demonstrate good potential for dual tunability in ferrite-ferroelectric bilayer thin films at microwave frequencies, and motivate their future use in phase shifters using discrete interdigital capacitors.

One of the authors (H.S.) acknowledges support from ARO Grant No. DAAD19-03-1-0277. The authors thank H.S. Nagaraja and R. Hyde for their help with the PLD system.

[1] *Magnetic Thin Film Devices* edited by J. D. Adam, Handbook of Thin Film Devices Vol. 4 (Academic, San Diego, 2000).
[2] *Ferroelectric Film Devices* edited by D. J. Taylor, Handbook of Thin Film Devices Vol. 5 (Academic Press, San Diego, 2000).
[3] M. J. Lancaster, J. Powell, and A. Porch, Supercond. Sci. Technol. **11**, 1323 (1998).
[4] C. Vittoria, J. Magn. Magn. Mater. **71**, 109 (1980).
[5] Q. X. Jia, J. R. Groves, P. Arendt, Y. Fan, A. T. Findikoglu, S. R. Foltyn, H. Jiang, and F. A. Miranda, Appl. Phys. Lett. **74**, 1564 (1999).
[6] W. J. Kim, W. Chang, S. B. Quadri, H. D. Wu, J. M. Pond, S. W. Kirchoefer, H. S. Newman, D. B. Chrisey, and J. S. Horwitz, Appl. Phys. A: Mater. Sci. Process. **71**, 7 (2000).
[7] G. Srinivasan, I. V. Zavislyak, and A. S. Tatarenko, Appl. Phys. Lett. **89**, 152508 (2006).
[8] S. R. Shinde, S. E. Lofland, C. S. Ganpule, S. B. Ogale, S. M. Bhagat, T. Venkatesan, and R. Ramesh, J. Appl. Phys. **85**, 7459 (1999).
[9] C. M. Carlson, T. V. Rivkin, P. A. Parilla, J. D. Perkins, D. S. Ginley, A. B. Kozyrev, V. N. Oshadchy, and A. S. Pavlov, Appl. Phys. Lett. **76**, 1920 (2000).
[10] J. C. Jiang, Y. Lin, C. L. Chen, C. W. Chu, and E. I. Meletis, J. Appl. Phys. **91**, 3188 (2002).
[11] P. A. Stampe, M. Bullock, W. P. Tucker, and R. J. Kennedy, J. Phys. D **32**, 1778 (1999).
[12] C. Klein, *Manual of Mineral Science*, 22nd ed. (Wiley, New York, 2002), pp. 17–200.
[13] S. E. Moon, E. K. Kim, S. J. Lee, M. H. Kwak, Y. T. Kim, H. C. Ryu, and W. J. Kim, Integr. Ferroelectr. **55**, 863 (2003).
[14] T. L. Hylton, M. A. Parker, K. R. Coffey, and J. K. Howard, J. Appl. Phys. **73**, 6257 (1993).
[15] X. Sui and M. H. Kryder, Appl. Phys. Lett. **63**, 1582 (1993).
[16] S. E. Moon, E. K. Kim, S. J. Lee, S. K. Han, K. Y. Kang, and W. J. Kim, Mater. Res. Soc. Symp. Proc. **720**, 79 (2002).
[17] C. L. Chen, J. Shen, S. Y. Chen, G. P. Luo, C. W. Chu, F. A. Miranda, F. W. Van Keuls, J. C. Jiang, E. I. Meletis, and H. Y. Chang, Appl. Phys. Lett. **78**, 652 (2001).